Journal of Nanoparticle Research

Caleosin-based nanoscale oil bodies for targeted delivery of hydrophobic anticancer drugs

--Manuscript Draft--

Manuscript Number:	NANO4661R1
Full Title:	Caleosin-based nanoscale oil bodies for targeted delivery of hydrophobic anticancer drugs
Article Type:	Original research
Keywords:	artificial oil body; caleosin; delivery carrier; Camptothecin
Corresponding Author:	Chung-Jen Chiang, Ph.D. China Medical University Taichung, TAIWAN, REPUBLIC OF CHINA
Corresponding Author Secondary Information:	
Corresponding Author's Institution:	China Medical University
Corresponding Author's Secondary Institution:	
First Author:	Chung-Jen Chiang, Ph.D.
First Author Secondary Information:	
All Authors:	Chung-Jen Chiang, Ph.D.
	Li-Jen Lin
	Chih-Jung Chen
All Authors Secondary Information:	
Manuscript Region of Origin:	
Abstract:	Nanoscale artificial oil bodies (NOBs) could be assembled from plant oil, phospholipids (PLs), and oleosin (Ole) as previously reported. NOBs have a lipid-based structure that contains a central oil space enclosed by a monolayer of Ole-bound PLs. As an oil structural protein, Ole functions to maintain the integrity of NOBs. Like Ole, caleosin (Cal) is a plant oil-associated protein. In this study, we investigated the feasibility of NOBs assembled by Cal for targeted delivery of drugs. Cal was first fused with anti-HER2/neu affibody (ZH2), and the resulting fusion gene (Cal-ZH2) was then expressed in Escherichia coli. Consequently, NOBs assembled with the fusion protein were selectively internalized by HER2/neu-positive tumor cells. The internalization efficiency could reach as high as 90%. Furthermore, a hydrophobic anticancer drug, Camptothecin (CPT), was encapsulated into Cal-based NOBs. These CPT-loaded NOBs had a size around 200 nm and were resistant to hemolysis. Release of CPT from NOBs at the non-permissive condition followed a sustained and prolonged profile. After administration of the CPT formulation, Cal-ZH2-displayed NOBs exhibited a strong antitumor activity toward HER2/neu-positive cells both in vitro and in vivo. The result indicates the potential of Cal-based NOBs for targeted delivery of hydrophobic drugs.
Response to Reviewers:	Dear Professor Yu: It is my pleasure to submit our revised manuscript (NANO4661) to Journal of Nanoparticle Research. An itemized list of changes addressing reviewers' comments is as follows. 1. As suggested, our preliminary results were summarized. See line 2-10, P. 4. 2. As suggested, a brief description of results was presented. See line 25-27, P. 4. 3. After resolution by sulfate-polyacrylamide gel electrophoresis (SDS-PAGE), Cal or Cal-ZH2 protein was isolated from SDS-PAGE as described previously. See line 16-18, P. 5. 4. The sonication condition for reconstitution of NOBs was set at 20 K Hz for 10 s with

	4. The sonication condition for reconstitution of NOBs was set at 20 K Hz for 10 s with an Ultrasonic Processor VCX750 (Sonics & Materials Co., USA). See line 21-22, P. 5. 5. Immunodetection was conducted by administration of the mouse anti-6xHis monoclonal antibody and followed by applying with the FITC-conjugated anti-mouse IgG anti-6xHis antibody. See line 6-9, P. 6. 6. PBS is sodium phosphate buffer as commonly used. See line 20-21, P. 5. 7. The confused sentence was rewritten: "CPT was analyzed with a Mightysil RP-18 GP column (Kanto, Japan) and detected with Waters 2996 Photodiode Arary Detector (Waters, USA)". See line 19-21, P. 7. 8. Centrifugation was performed at 600 g. See line 9, P. 8. 9. The hemolytic activity was determined with the reference to blank (erythrocytes treated with PBS) and completely hemolyzed samples (distilled water). See line 10-12, P. 8. 10. Animal experiments were carried out by complying with the principles outlined by the Ethics Committee on Animal Experimentation at China Medical University (protocol no. 99-18-N). See line 15-19, P. 8. 11. “…various pharmacokinetics…” was changed to “…variable pharmacokinetics…”. See line 15, P. 11. 12. The description was changed to “a high zeta potential (|measured value| > 30 mV) of Cal-based NOBs”. See line 19-21, P.11. 13. As suggested, Fig. 6D was placed in the inset of Fig. 6C. Fig. 6D was therefore removed. 14. Conclusion section was rewritten as suggested. See line 26, P. 13; line 1-13, P. 14. I would love to acknowledge reviewers for their valuable comments. Your kind suggestions on our work are greatly appreciated as well. Best regards, Chung-Jen Chiang Assistant Professor Department of Medical Laboratory Science and Biotechnology China Medical University

Caleosin-based nanoscale oil bodies for targeted delivery of hydrophobic anticancer drugs

Chung-Jen Chiang[1,*], Li-Jen Lin[2], and Chih-Jung Chen[1]

[1] Department of Medical Laboratory Science and Biotechnology, China Medical University, 91 Hsue-Shih Road, Taichung 40402, Taiwan

[2] School of Chinese Medicine, China Medical University, Taichung, Taiwan

* Corresponding author

Phone: 886-4-22003366 ext. 7227; FAX: 886-4-22057414.

E-mail address: cjchiang@mail.cmu.edu.tw

Abstract

Nanoscale artificial oil bodies (NOBs) could be assembled from plant oil, phospholipids (PLs), and oleosin (Ole) as previously reported. NOBs have a lipid-based structure that contains a central oil space enclosed by a monolayer of Ole-bound PLs. As an oil structural protein, Ole functions to maintain the integrity of NOBs. Like Ole, caleosin (Cal) is a plant oil-associated protein. In this study, we investigated the feasibility of NOBs assembled by Cal for targeted delivery of drugs. Cal was first fused with anti-HER2/*neu* affibody (ZH2), and the resulting fusion gene (Cal-ZH2) was then expressed in *Escherichia coli*. Consequently, NOBs assembled with the fusion protein were selectively internalized by HER2/*neu*–positive tumor cells. The internalization efficiency could reach as high as 90%. Furthermore, a hydrophobic anticancer drug, Camptothecin (CPT), was encapsulated into Cal-based NOBs. These CPT-loaded NOBs had a size around 200 nm and were resistant to hemolysis. Release of CPT from NOBs at the non-permissive condition followed a sustained and prolonged profile. After administration of the CPT formulation, Cal-ZH2-displayed NOBs exhibited a strong antitumor activity toward HER2/*neu*-positive cells both *in vitro* and *in vivo*. The result indicates the potential of Cal-based NOBs for targeted delivery of hydrophobic drugs.

Keywords: artificial oil body, caleosin, delivery carrier, Camptothecin

Introduction

Targeted therapy is well recognized as one of the most promising methods for cancer treatment (Farokhzad and Langer 2009). A typical approach commonly implements a drug-loaded vehicle conjugated with a bioactive ligand that specifically binds to the tumor cell-specific biomarker. As a consequence of targeting, the chemotherapeutic drug can be delivered to cancerous sites to prevent the detrimental side-effect from normal cells (Cho et al. 2008). However, many known anticancer pharmaceuticals of high potency are poorly soluble. Administration of these hydrophobic drugs loaded-carriers in an oral or intravenous way usually causes many problems, such as low bioavailability and aggregate deposition of pharmaceuticals at the local site (Fernandez et al. 2001; Lipinski et al. 2000). Obviously, it renders formulations of hydrophobic drugs for efficient administration challenging.

A myriad of drug carrier systems at a nano scale have been developed for targeted delivery of pharmaceuticals (Andresen et al. 2005; Torchilin 2005; Zhang et al. 2008). One advantage of nanocarriers is to improve the pharmacokinetic properties and therapeutic index of drugs (Ferrari 2005). Among many nanocarriers, liposome and polymeric micelle are two prominent examples for formulation of hydrophobic agents. However, optimization of many biophysicochemical parameters still complexes the drug formulations with these two carriers (Andresen et al. 2005; Torchilin 2007). Recently, we have sought to an alternative and explored artificial oil bodies (AOBs) as a novel delivery vehicle (Chiang et al. 2010; Chiang et al. 2011). Technically, AOBs are assembled in one step by sonicating the mixture containing plant oil, phospholipids (PLs), and oleosin (Ole). AOBs resemble their natural counterpart, plant seed oil body (OB), and consist of the triacylglycerol (TAG) matrix (see Fig. 1). The TAG is covered by a monolayer of PLs associated with the structural protein, Ole. Ole has a central lipophilic core that is embedded into PLs and two terminal domains protruded outwards (Huang 1996; Napier et al. 1996). The two arms provide the electronegative repulsion force, thereby making Ole-based AOBs stable

and intact (Tzen et al. 1992).

In our preliminary work, nanoscale AOBs (NOBs) was obtained by tailoring the ratio of Ole to oil (Chiang et al. 2010; Chiang et al. 2011). Moreover, NOBs were made functional by displaying the arginine-glycine-aspartic acid (RGD) motif or a bivalent anti-HER2/*neu* affibody (denoted as ZH2) on their surface. As encapsulated with a hydrophobic dye, these RGD- or ZH2-displayed NOBs could selectively penetrate tumor cells overexpressing $\alpha_v\beta_3$ integrin and HER2/*neu*, respectively. These dye-loaded NOBs were sensitive to low pH and disintegrated over time after entry into acidic endosomes of tumor cells, thus leading to release the cargo dye. Overall, these results indicate the potential of NOBs as a targeted delivery carrier.

Like Ole, caleosin (Cal) is an OB-associated protein but plays a distinct role (Chen et al. 1999). Both Ole and Cal share structural similarity (Frandsen et al. 2001). Interestingly, replacement of Ole with Cal to assemble AOBs resulted in a smaller size and higher stability (Liu et al. 2009). NOBs essentially contain a hydrophobic core, which makes them very appealing for encapsulation of hydrophobic drugs. Therefore, this study was aimed to investigate the feasibility of Cal-based NOBs for targeted delivery of insoluble drugs. Tumor cells with the HER2/*neu* biomarker were chosen for targeting. HER2/*neu* belongs to the human epidermal growth factor receptor family (Hung and Lau 1999). Abnormal overexpression of HER2/*neu* can lead to the progression of aggressive tumors (Citri and Yarden 2006). To make NOBs functional, Cal was fused with ZH2 (Cal-ZH2). A single domain of ZH2 consisting of 58 amino acid residues is derived from one of the IgG-binding domain of staphylococcal protein A. This small motif displays a high binding affinity to the extracellular domain of HER2/*neu* (Orlova et al. 2006). After overproduction in *Escherichia coli*, Cal-ZH2 was recovered to assemble NOBs. As a result of entrapment with a hydrophobic antitumor drug, Camptothecin (CPT), Cal-based NOBs exhibited a strong antitumor activity both *in vitro* and *in vivo*. The result indicates the potential of Cal-based NOBs for targeted delivery of water-repelling drugs.

Experimental procedures

DNA manipulation and bacterial culturing

The ZH2 motif was recovered from plasmid pBlue-ZH2 (Chiang et al. 2011) by *EcoR*V-*Hind*III cleavage. The recovered DNA fragment was then incorporated into plasmid pET29a-Cal (Chen et al. 2004) to give plasmid pJO1-Cal-ZH2. This plasmid construction resulted in the Cal-ZH2 fusion under the control of the T7 promoter. In addition, plasmid pET29a-Cal contained the T7 promoter-driven Cal along and served as a control. After transformation of pJO1-Cal-ZH2 and pET29a-Cal, *E. coli* strain BL21(DE3) were cultured in shake flasks containing Luria-Bertani (LB) medium (Miller 1972). Bacterial cultures were maintained at 37^{o}C and induced with 100 μM IPTG for protein production.

Self-assembly of NOBs

Assembly of NOBs essentially followed the previous method (Chiang et al. 2011). In brief, proteins expressed in *E. coli* were resolved by sulfate-polyacrylamide gel electrophoresis (SDS-PAGE) and isolation of Cal or Cal-ZH2 from SDS-PAGE was preformed as described previously (Chuang et al. 1996). Unless stated otherwise, the assembly solution (1 mL) was prepared by mixing 100 μg of olive oil, 150 μg of PLs, and 500 μg of isolated Cal or Cal-ZH2 fusion protein in sodium phosphate buffer (PBS) at pH 7.5. The mixture was then subjected to sonication at 20 K Hz for 10 s with an Ultrasonic Processor VCX750 (Sonics & Materials Co., USA). Sonication was repeated three times on ice. After centrifugation, AOBs were collected from the top and washed with PBS. To encapsulate the hydrophobic dye or drug, NOBs were assembled in a similar manner except that 1 μg yellow GGK dye (Widetex Co., Taiwan) or 500 μg CPT was additionally added to the assembly solution. Plant oils utilized here were soybean oil (Taiwan Sugar Co., TW), peanut oil (Leader Price Co., TW), sesame oil (Taisun Co., TW), olive oil (Taisun Co., TW), and mineral oil (Sigma, MO).

Immunoassay

The 6xHis tag on the surface of NOBs was detected by the immunoassay as reported previously (Chiang et al. 2011). NOBs were fixed in 2.5% (w/v) paraformaldehyde and soaked in a solution containing 3 % BSA in PBS at room temperature. Immunodetection was then conducted by administration of the mouse anti-6xHis monoclonal antibody (Genemark technology Co. ltd, Taiwan) and followed by applying with the FITC-conjugated anti-mouse IgG anti-6xHis antibody (Jackson Immuno Research, USA). After color development with 3mM 4-chloro-1-naphthol, NOBs were mounted on glass slides for observation by fluorescence microscopy (Olympus IX71, Japan).

Morphology, size, and stability of NOBs

Essentially following the previous report (Chiang et al. 2011), NOBs were characterized with respect to their morphology, size, and stability. The analyses were carried out using transmission electron microscopy (TEM) (Jeol JEM-1400, Japan), N4-submicron particle size analyzer (Beckman Coulter, USA), and spectrophotometer (Beckman DU530, USA), respectively.

Microscopy and flow cytometry

According to the previous report (Chiang et al. 2011), human cancer cell lines, MDA-MB-231 (ovarian), SKOV3 (ovarian), MCF7 (breast) and MCF7/Her18 (HER2-transfected stable cell line), were cultivated and processed for treatment with NOBs. At the end of treatment, the HER2/*neu* receptor of cells was detected with anti-HER2/*neu* antibody (Santa Cruz Biotech., USA) that was against with anti-mouse IgG-TRIAC (Jackson ImmunoResearch Lab., USA). Meanwhile, cell nuclei were stained by diamidino-2-phenylindole (DAPI). Cells were then observed with fluorescence microscopy (Olympus IX71, Japan) and confocal microscopy (Leica TCS SP2, Germany). Furthermore, internalized NOBs were analyzed using a

FACScanto flow cytometer system (Becton Dickinson, USA).

Fourier transform infrared spectroscopic (FTIR) analysis

The CPT formulations with NOBs were analyzed on KBr pellets with the DIGILAB FTS3500 spectrophotometer (Bio-Rad, USA). The FTIR spectra were collected in the region from 4000 cm^{-1} to 650 cm^{-1}.

Differential Scanning Calorimetry (DSC)

The DSC themograms of CPT formulations with NOBs were analyzed using a CSC 6300 microcalorimeter (Calorimetry Science Co. USA) with a heating rate of 10^{o}C/min. The melting point and heat of fusion were calibrated based on Indium. Relative to an empty pan, the aluminum sample pan (Calorimetry Science Co.) was employed as a standard.

Drug release study *in vitro*

Placed in a dialysis bag (Spectrum Laboratories, USA), CPT-loaded NOBs (1 mL) were immersed in 20 mL of 0.01 M PBS. The dialysis was conducted at 37^{o}C under constant stirring. At time intervals, aliquots of PBS (100 μL) were withdrawn to determine CPT by high performance liquid chromatography (HPLC). CPT was analyzed with a Mightysil RP-18 GP column (Kanto, Japan) and detected with Waters 2996 Photodiode Arary Detector (Waters, USA). The mobile phase consisting of acetonitrile and water (30:70) was pumped at 1 mL/min and the detection was set at 254 nm. The released content of CPT in PBS was normalized to the weight that was initially encapsulated in NOBs. All experiments were conducted in triplicate.

In vitro assessment of cytotoxicity

Tumor cells cultured in a 96-well plate were administrated with the CPT formulations.

After the treatment, the supernatant was removed and cells were washed with PBS. On the basis of the cell-counting kit (Dojindo Molecular Technologies, Inc.), the absorbance of cells in each well was measured at 450 nm with a microplate reader (SpectraMax M2, Molecular Device, USA). Cell viability was defined as the ratio of absorbance for NOBs-treated cells to that for untreated cells.

Hemolysis assay

CPT-loaded NOBs were incubated in diluted blood (1 mL) at 37^{o}C for 30 min. After centrifugation at 600 g for 3 min, released hemoglobin was measured at 543 nm with a spectrophotometer. The hemolytic activity was determined with the reference to blank (erythrocytes treated with PBS) and completely hemolyzed samples (distilled water).

Antitumor activity *in vivo*

Animal experiments were carried out by complying with the principles outlined by the Ethics Committee on Animal Experimentation at China Medical University (protocol no. 99-18-N). BALB/cAnN.Cg nude mice (4 weeks old, female, and 20 g body weight) were purchased from the National Laboratory Animal Center in Taiwan and maintained in the Animal Center at China Medical University. SKOV3 cells (1×10^{7}) in 0.1 mL PBS were injected into the right flank of nude mice. The CPT formulations were administrated by two intratumorous injections (on day 1 and day 5) per week when the volume of tumor nodules was >150 mm^{3}. Tumor-bearing mice were randomly assigned to 4 groups, and there were 5 mice for each group. The body weight and tumor volume of mice were then measured twice weekly. The length and width of tumor modules were measured with a caliper to calculate the tumor volume based on the following equation:

Tumor volume (V) = length×width×width/2

Results and discussion

Self-assembly of Cal-based NOBs

Plasmid pJO1-Cal-ZH2 was constructed to contain the C-terminal fusion of Cal with ZH2 (Cal-ZH2). This plasmid construction also created a 6xHis tag appended to the C-terminus of Cal-ZH2. Meanwhile, plasmid pJO1-Cal contained Cal alone and served as the control herein. It is recognized that monoclonal antibody has a large size such that it can be easily taken up by liver and exhibits poor tissue penetration (Steffen et al. 2006). In contrast, ZH2 is an affibody of small size, which offers an advantage for administration in terms of efficacy.

The protocol for preparing NOBs was outlined in Fig. 1. After overproduction in *E. coli*, either insoluble Cal-ZH2 or Cal was recovered and then mixed with olive oil, PL, and a hydrophobic dye. By sonication, NOBs self-assembled in one step and floated on the top of supernatant after centrifugation. The immunoassay was conducted to analyze NOBs using the anti-6xHis tag antibody. As shown in Fig. 2, NOBs prepared from Cal-ZH2 or Cal had a comparable nanoscale size and emitted green fluorescence. This indicates the encapsulation of the hydrophobic dye into NOBs. Moreover, the red fluorescence was only detected in NOBs assembled with Cal-ZH2 whereas the signal was absent in Cal-based NOBs. The result suggests the functional display of the 6xHis tag via Cal on the surface of NOBs.

Tunable size of Cal-based NOBs

As reported previously (Chiang et al. 2011), the size of NOBs was tunable in response to three factors, including plant oil, weight ratio of plant oil to protein, and pH. To investigate the factor effect, NOBs were first assembled using various plant oils at pH 7.5. The weight ratio of oil to Cal-ZH2 (O/P) was set at 1:1. Consequently, apart from

mineral oil, NOBs prepared from other oils remained integral and had a small size around 400 nm (Table 1). This result implies that the TAG composition of assorted oils likely has a various degree of interaction with Cal-ZH2.

Olive oil was chosen to examine the effect of the O/P ratio on NOBs at pH 7.5. As a consequence, NOBs had a smaller size at a lower O/P ratio (Table 1). The size of NOBs was smaller than 200 nm when the O/P ratio was below 1. More Cal-ZH2 than oil in the NOBs formulation indicates that more terminal domains of Cal are exposed, which elicits a stronger steric repulsion force. Therefore, this would contribute to high stability of NOBs.

Finally, the effect of pH on NOBs was assessed with the O/P ratio at 1:1. The pH value higher than 6.5 was chosen for assessment because NOBs were sensitive to acidity (Chiang et al. 2011). As a result, the size of NOBs was in the range of 370-450 nm (Table 1). However, NOBs had a size above 600 nm at acidic pH. It is likely that the electronegative repulsion force provided by Cal in NOBs is diminished due to neutralization by proton ions under the acid condition.

Selective internalization of ZH2-displayed NOBs

To examine the functionality of ZH2, NOBs encapsulated the hydrophobic dye were applied to various tumor cells. As shown in Fig. 3A, HER2/*neu*-overexpressing cells (e.g., MCF7/Her18 and SKOV3) emitted the strong fluorescence whereas the signal was absent in the HER2/*neu*-negative cells (e.g., MCF7 and MDA-MB-231). Regardless of cell types, no signals could be detected with NOBs free of displayed ZH2 (e.g. assembled with Cal alone). These results suggest functional display of the ZH2 motif on the surface of NOBs, which in turn leads these oil particles to selective targeting of HER2/*neu*-positive cells. Moreover, Fig. 3B shows that the blue signals of stained lysosomes co-localized mostly with the green fluorescence emitted by NOBs. The result indicates that the internalized NOBs are located inside the cell lysosomes.

The internalization efficiency of NOBs was further determined by counting the

percentage of fluorescence-emitting cells in the whole cell population. Flow cytometry shows that the percentage of cells emitting green fluorescence generally increased with the increasing NOBs dose (Fig. 3C). With the dose exceeding 12.5 μg/mL, more than 90% of HER2/*neu*-positive cells (e.g., MCF17/Her18 and SKOV3) could emit green fluorescence after exposure to Cal-based NOBs for 2 h. This result indicates that Cal-based NOBs is superior to Ole-based NOBs in terms of internalization efficiency (Chiang et al. 2011).

Characterization of drug-loaded NOBs

As illustrated above, Cal-based NOBs were effective for selective targeting of HER2/*neu*-positive cells. It was intuitive to investigate the usefulness of these NOBs for targeted delivery of hydrophobic drugs. First identified in *Camptotheca acuminate*, CPT is a cytotoxic alkaloid that inhibits the activity of topoisomerase I during the cell cycle (Shao et al. 1997). This toxic drug is poorly absorbed by oral administration and exhibits variable pharmacokinetics (Garcia-Carbonero and Supko 2002; Soepenberg et al. 2003). Therefore, CPT was chosen for formulation with NOBs. As analyzed by TEM, NOBs had a spherical size around 200 nm (Fig. 4A), in agreement with that measured by the laser light scattering (Table 2). In generally, loading of CPT had an insignificant effect on the size of and the zeta potential of NOBs. A high zeta potential (|measured value| **>** 30 mV) of Cal-based NOBs implies that they are relatively stable as suggested previously (Lee et al. 2007; Suthiwangcharoen et al. 2011). Meanwhile, plain CPT gave a characteristic melting peak at 270^{o}C based on the DSC assay. This endothermic peak was absent from the DSC thermogram for CPT that was encapsulated into NOBs (Figure 4B). This suggests that CPT is dispersed in NOBs (Barreiro-Iglesias et al. 2004).

In addition, the FTIR analysis (Fig. 4C) shows that plain NOBs exhibited main

characteristic peaks at 2954, 2920 and 2852 cm^{-1} (C–H stretching vibrations), 1749 cm^{-1} (C=O stretching vibration), 1463cm^{-1} (C–H deformation) and 721 or 723 cm^{-1} $(CH_2)_n$, (n>4) bonding (Lacey et al. 1998). The FTIR spectra of CPT alone gave the most prominent bands at 2954 and 2852 cm^{-1} (C-H), 1745 and 1652cm^{-1} (C=O stretching vibration of ester and lactone carbonyl group), and 1163cm^{-1} (C-N stretching vibration of benzene ring). In general, the characteristic peaks of CPT still appeared in the spectrum once CPT was encapsulated into NOBs (e.g., F50 and F500), and no new peaks occurred. This suggests an insignificant interaction between CPT and NOBs (Wenkai et al. 2003), which is consistent with the DSC result.

As depicted in Fig. 5, release of CPT from NOBs followed a sustained and prolonged drug release profile. An initial burst release of CPT occurred in the first 5 h. Consequently, the released amount accounted for 60%, 45% and 25% of original CPT for F50, F100, and F500 formulations, respectively.

In vitro cytotoxicity study and hemolysis test

The cytotoxic effect of CPT formulations on the cells was first assessed *in vitro*. Fig. 6A shows that ZH2-displayed NOBs free of CPT were biocompatible with cells. Upon encapsulation of CPT, these NOBs could reduce the viability of HER2/*neu*-positive cells but were harmless to HER2/*neu*-negative cells. Moreover, the degree of this cytotoxicity effect was correlated with the CPT dose. As illustrated above, ZH2-displayed NOBs could be selectively internalized by HER2/*neu*-positive cells. Therefore, the observed cytotoxic effect is attributed to targeted delivery of CPT into HER2/*neu*-positive cells via functional NOBs. Note that plain CPT could exhibit a non-specific cytotoxicity. In addition, the CPT dose in the form of NOBs formulation that reduces cell viability by 50% was estimated to be 45 and 70 μg/mL for SKOV3 and MCF17/Her18 cells, respectively (Fig. 6B).

The hemolysis test for NOBs was further conducted. After incubated with CPT-loaded NOBs, erythrocytes remained unaffected (Fig. 6C). Further analysis shows that no blood cell agglutination occurred (Fig. 6B). Overall, these results indicate the potential safety of NOBs.

In vivo antitumor activity

At last, the *in vivo* antitumor activity of CPT-loaded NOBs was evaluated in a xenograft animal model. The drug formulations were prepared by encapsulation of CPT into ZH2-free NOBs (NOB-CPT) and ZH2-displayed NOBs (ZH-NOB-CPT). As shown in Fig. 7A, the xenograft tumors without any treatment (control) grew uncontrollably whereas they regressed with time after receiving the treatment of ZH-NOB-CPT. At the end, the average tumor size was reduced to 20% of the initial volume. Upon administration of the NOB-CPT formulation, the average tumor volume was increased by 25%. In contrast, administration of plain CPT gave a marginal antitumor activity and the tumor volume was increased by 10% at the end. These results indicate that the cytotoxic effect of CPT could be sheltered as the drug is encapsulated into NOBs lacking ZH2 (e.g., the NOB-CPT formulation).

In addition, Fig. 7B shows that the change in the body weight of tumor-bearing mice was insignificant for the treatment with the ZH-NOB-CPT or NOB-CPT formulations. Receiving PBS (control), mice gained 10% of the original weight that the size of their xenograft tumors were doubled (Fig. 7A). Administrated with plain CPT, the weight of mice was reduced by 20%.

Conclusions

NOBs comprise a central oil core enclosed by Cal-bound lipid monolayer (Fig. 1). By

surface display of a bioactive motif (e.g., ZH2) linked to Cal, NOBs could be selectively internalized into HER2/*neu*-positive cells. In addition, the two protruding domains of Cal provide the electronegative surface charge that prevents NOBs from association with non-target cells. Indeed, CPT is hydrolytically instable and has adverse drug interaction. Many efforts have been devoted to the development of intralipid formulations of CPT (Venditto and Simaneck 2010), such as using liposomes and polymeric micelles (Elbayoumi et al. 2007; Shmeedaa et al. 2009; Sugarman et al. 1996). As illustrated here, the pharmacokinetic property of CPT could be improved as formulated with Cal-based NOBs. Administration of these CPT-loaded NOBs exhibited a strong antitumor activity on HER2/*neu*-positive tumor cells both *in vitro* and *in vivo*. In summary, Cal-based NOBs are featured with biocompatibility, reproducibility, and small size, thus appearing to be a potential delivery carrier for hydrophobic drugs.

Acknowledgements

This work was supported by National Science Council of Taiwan (NSC 99-2313-B-039-003-MY3), China Medical University (CMU100-S-29), and Ministry of Economic Affairs (99-EC-17-A-10-S1-156).

References

Andresen TL, Jensenb SS, Jørgensen K (2005) Advanced strategies in liposomal cancer therapy: problems and prospects of active and tumor specific drug release Prog Lipid Res 44:68-97.

Barreiro-Iglesias R, Bromberg L, Temchenko M, Hatton TA, Concheiro A, Alvarez-Lorenzo C (2004) Solubilization and stabilization of camptothecin in micellar solutions of pluronic-*g*-poly(acrylic acid) copolymers. J Control Release 97:537-549.

Chen JC, Tsai CC, Tzen JTC (1999) Cloning and secondary structure analysis of caleosin, a unique calcium-binding protein in oil bodies of plant seeds. Plant Cell Physiol 40:1079-1086.

Chen MC, Chyan CL, Lee TT, Huang SH, Tzen JTC (2004) Constitution of stable artificial oil bodies with triacylglycerol, phospholipid, and caleosin. J Agri Food Chem 52:3982-3987.

Chiang CJ, Chen CJ, Chang CH, Chao YP (2010) Selective delivery of cargo entities to tumor cells by nanoscale artificial oil bodies. J Agri Food Chem 58:11695-11702.

Chiang CJ, Lin LJ, Lin CC, Chang CH, Chao YP (2011) Selective internalization of self-assembled artificial oil bodies by HER2/neu-positive cells. Nanotechnol 22:015102.

Cho K, Wang X, Nie S, Chen Z, Shin DM (2008) Therapeutic nanoparticles for drug delivery in cancer. Clin Cancer Res 14:1310-1316.

Chuang RLC, Chen JCF, Chu J, Tzen JTC (1996) Charcterization of seed oil bodies and their surface oleosin isoforms from rice embryos. J Biochem 120:74-81.

Citri A, Yarden Y (2006) EGF-ERBB signalling: towards the systems level. Nat. Rev. Mol. Cell Biol. 7:505-516.

Elbayoumi TA, Pabba S, Roby A, Torchilin VP (2007) Antinucleosome antibody-modified liposomes and lipid-core micelles for tumor-targeted delivery of therapeutic and diagnostic agents. J Liposome Res 17:1-14.

Farokhzad OC, Langer R (2009) Impact of nanotechnology on drug delivery. ACS Nano 3:16-20.

Fernandez AM, Van derpoorten K, Dasnois L, Lebtahi K, Dubois V, Lobl TJ, Gangwar S, Oliyai C, Lewis ER, Shochat D and others (2001) N-Succinyl-(β-alanyl-l-leucyl-l-alanyl-l-leucyl)doxorubicin: an extracellularly tumor-activated prodrug devoid of intravenous acute toxicity J Med Chem 44:3750-3753.

Ferrari M (2005) Nanotechnology: opportunities and challenges. Nat. Rev. Cancer

5:161-171.

Frandsen GI, Mundy J, Tzen JTC (2001) Oil bodies and their associated proteins, oleosin and caleosin Physiol Plant 112:301-307.

Garcia-Carbonero R, Supko JG (2002) Current perspectives on the clinical experience, pharmacology, and continued development of the Camptothecins. Clin Cancer Res 8:641-661.

Huang AH (1996) Oleosins and oil bodies in seeds and other organs. Plant Physiol 110:1055-1061.

Hung MC, Lau YK (1999) Basic science of HER2/*neu*: a review. Semin. Oncol. 26:51-59.

Lacey DJ, Wellner N, Beaudoin F, Napier JA, Shewry PR (1998) Secondary structure of oleosins in oil bodies isolated from seeds of safflower (*Carthamus tinctorius* L.) and sunflower (*Helianthus annuus* L.). Biochem J 334:469-477.

Lee HK, Lee HY, Jeon JM (2007) Codeposition of micro- and nano-sized SiC particles in the nickel matrix composite coatings obtained by electroplating. Surf Coat Tech 201:4711-4717.

Lipinski CA, Lombardo F, Dominy BW, Feeney PJ (2000) Experimental and computational approaches to estimate solubility and permeability in drug discovery and development settings Adv Drug Deliv Rev 46:3-36.

Liu TH, Chyan CL, Li FY, Tzen JTC (2009) Stability of artificial oil bodies constituted with recombinant caleosins J Agri Food Chem 57:2308-2313.

Miller JH (1972) Experiments in molecular genetics. Cold Spring Harbor, New York: Cold Spring Harbor Laboratory.

Napier JA, Stobart AK, Shewry PR (1996) The structure and biogenesis of plant oil bodies: the role of the ER membrane and the oleosin class of proteins. Plant Mol Biol 31:945-956.

Orlova A, Magnusson M, Eriksson TLJ, Nilsson M, Larsson B, Hoiden-Guthenberg I, Widstrom C, Carlsson J, Tolmachev V, Stahl S and others (2006) Tumor imaging using a picomolar affinity HER2 binding affibody molecule. Cancer Res. 66:4339-4348.

Shao RG, Cao CX, Shimizu T, O'Connor PM, Kohn KW, Pommier Y (1997) Abrogation of an S-phase checkpoint and potentiation of Camptothecin cytotoxicity by 7-hydroxystaurosporine (UCN-O1) in human cancer cell lines, possibly Influenced by p53 function. Cancer Res 57:4029-4035.

Shmeedaa H, Tzemacha D, Maka L, Gabizon A (2009) Her2-targeted pegylated liposomal doxorubicin: retention of target-specific binding and cytotoxicity after *in vivo* passage. J Control Release 136:155-160.

Soepenberg O, Sparreboom A, Verweij J (2003) The Alkaloids: clinical studies of Camptothecin and derivatives. Chem Biol 60:1-50.

Steffen AC, Orlova A, Wikman M, Nilsson FY, Ståhl S, Adams GP, Tolmachev V, Carlsson J (2006) Affibody-mediated tumour targeting of HER-2 expressing xenografts in mice. Eur J Nucl Med Mol Imaging 33:631-638.

Sugarman SM, Zou YY, Wasan K, Poirot K, Kumi R, Reddy S, Perez-Soler R (1996) Lipid-complexed camptothecin: formulation and initial biodistribution and antitumor activity studies Cancer Chemother Pharmacol 37:531-538.

Suthiwangcharoen N, Li T, Li K, Thompson P, You S, Wang Q (2011) M13 bacteriophage-polymer nanoassemblies as drug delivery vehicles Nano Res 4:483-493.

Torchilin VP (2005) Lipid-core micelles for targeted drug delivery. Curr Drug Deliv 2:319-327.

Torchilin VP (2007) Micellar nanocarriers: pharmaceutical perspectives. Pharm Res 24:1-16.

Tzen JTC, Lie GC, Huang AH (1992) Characterization of the charged components and their topology on the surface of plant seed oil bodies J Biol Chem 267:15626-15634.

Venditto VJ, Simaneck EE (2010) Cancer therapies utilizing the Campothcins: a review of the in vivo literature. Mol Pharma 7:307-349.

Wenkai T, Wang L, D'Souza MJ (2003) Evaluation of PLGA microspheres as delivery system for antitumor agent-Camptothecin. Drug Dev. Ind. Pharm. 29:745-756.

Zhang L, Chan JM, Gu FX, Rhee JW, Wang AZ, Radovic-Moreno AF, Alexis F, Langer R, Farokhzad OC (2008) Self-assembled lipid-polymer hybrid nanoparticles: a robust drug delivery platform. ACS Nano 8:1696-1702.

Figure
Click here to download Figure: CalZH-Fig-2.doc

Table 1. Size of Cal-based NOBs assembled at various (A) plant oils, (B) O/P ratios, and (C) pHs.

(A)		(B)		(C)	
oil	Mean particle size (nm)	O/P ratio (w/w)	Mean particle size (nm)	pH	Mean particle size (nm)
mineral oil	836.7 ± 12.7*	10:1	1273.6 ± 48.5	6.5	634.0 ± 24.1
soybean oil	463.1 ± 8.2	2:1	843.2 ± 53.1	7.0	693.5 ± 30.1
peanut oil	430.1 ± 7.7	1:1	466.6 ± 64.4	7.5	466.6 ± 64.4
olive oil	466.6 ± 64.4	1:5	163.9 ± 26.2	8.0	403.9 ± 48.0
sesame oil	431.5 ± 67.4	1:10	87.4 ± 51.2	9.0	372.0 ± 59.5

*Each data point represents the mean ± standard deviation from three independent measurements.

Table 2. Particle size and surface charge measurements of Cal-based NOBs encapsulated with various CPT concentrations.

Formulation	(A) Mean particle size (nm)	(B) Zeta-potential (mV)
NOBs	163.9 ± 26.2*	-49.1 ±2.5
F50	218.6 ± 50.5	-45.5 ± 3.2
F500	232.6 ± 67.6	-43.2 ± 2.2

*Each data point represents the mean ± standard deviation from three independent measurements.

Figure legend

Figure 1. The illustrative scheme outlining the protocol for administration of self-assembled NOBs. First, a hybrid fusion was generated by in-frame fusion of Cal with a bioactive ligand (e.g., ZH2). Second, overexpression of the hybrid gene in *E. coli* resulted in the inclusion body. Third, the insoluble protein was isolated and mixed with TAG (plant oil), PL, and a hydrophobic drug (e.g., CPT). Upon sonication, NOBs underwent self-assembly in one step. Finally, *in vitro* and *in vivo* antitumor activities were assessed by administration of drug-loaded NOBs.

Figure 2. Immunodetection of the 6xHis tag displayed onto NOBs. Encapsulated with the hydrophobic dye (green), NOBs were assembled with Cal (upper) or Cal-ZH2 (bottom). Immnodetection of 6xHis tag on NOBs' surface was conducted with the antibody against the tag (red). The scale bar equals 2 μm.

Figure 3. Internalization of NOBs by tumor cells. (A) Analysis of internalized NOBs by fluorescence microscopy. Encapsulated with the hydrophobic dye (green), NOBs assembled with Cal-ZH2 (upper) or Cal (bottom) were applied to tumor cells. For clear observation, cell nuclei (blue) and the HER2/*neu* receptor (red) were stained by DAPI and anti-HER2/*neu* antibody, respectively. The individual images were taken and then merged. The scale bar equals 20 μm. (B) Analysis of the cellular location of internalized NOBs. After incubation with ZH2-displayed NOBs carrying the dye (green), SKOV3 cells were stained with LysoSensor green DND-167. Consequently, cell lysosomes were stained blue and observed by Confocal microscopy. Overlaying the two images gave the panel shown on the right. (C) Analysis of internalization efficiency by flow cytometry. Tumor cells were co-incubated with various doses of ZH2-displayed NOBs carrying the fluorescent dye for 2 h. After washing, treated tumor cells were processed for flow cytometry analysis. The experiment was performed in triplicate.

Figure 4. Characterization of NOBs. Cal-ZH2-based NOBs were assembled with the O/P ratio at 1:5 and pH 7.5. To encapsulate the drug, an indicated amount of CPT was additionally added to the assembly solution. (A) TEM images of NOBs loaded with (F500, right panel) or without CPT (left panel). (B) DSC thermograms of CPT formulations. (C) FTIR spectrum of CPT formulations. Symbols: CPT, plain CPT; NOBs, NOBs without CPT; F50, NOBs loaded with 50 μg/mL CPT; F500, NOBs loaded with 500 μg/mL CPT.

Figure 5. Drug release profile of NOBs. CPT was loaded into NOBs with the concentration of 50 (F50), 100 (F100), and 500 μg/mL (F500). Consequently, CPT-loaded NOBs were analyzed for the drug release. The experiment was conducted in triplicate.

Figure 6. *In vitro* antitumor activity of and safety of CPT-loaded NOBs. (A) The viability of various cells receiving the CPT formulations. Plain CPT (500 μg/mL) in olive oil was used as a control. The experiment was conducted in triplicate. Refer to Figure 4 for the symbols used. (B) Correlation of cell viability with the CPT dose. (C) Hemolysis of erythrocyts with various CPT formulations. Saline was used as a negative control while distilled water as a positive control. Inset: photographs of erythrocytes after incubation with various CPT formulations.

Figure 7. *In vivo* antitumor activity of CTP-loaded NOBs. Tumor-bearing mice (n=5) were injected with CPT-loaded NOBs as described. (A) Regression rate of tumor volume after administration of CPT formulations. PBS was used as a negative control. (B) Body weight change of mice after administration of CPT formulations.

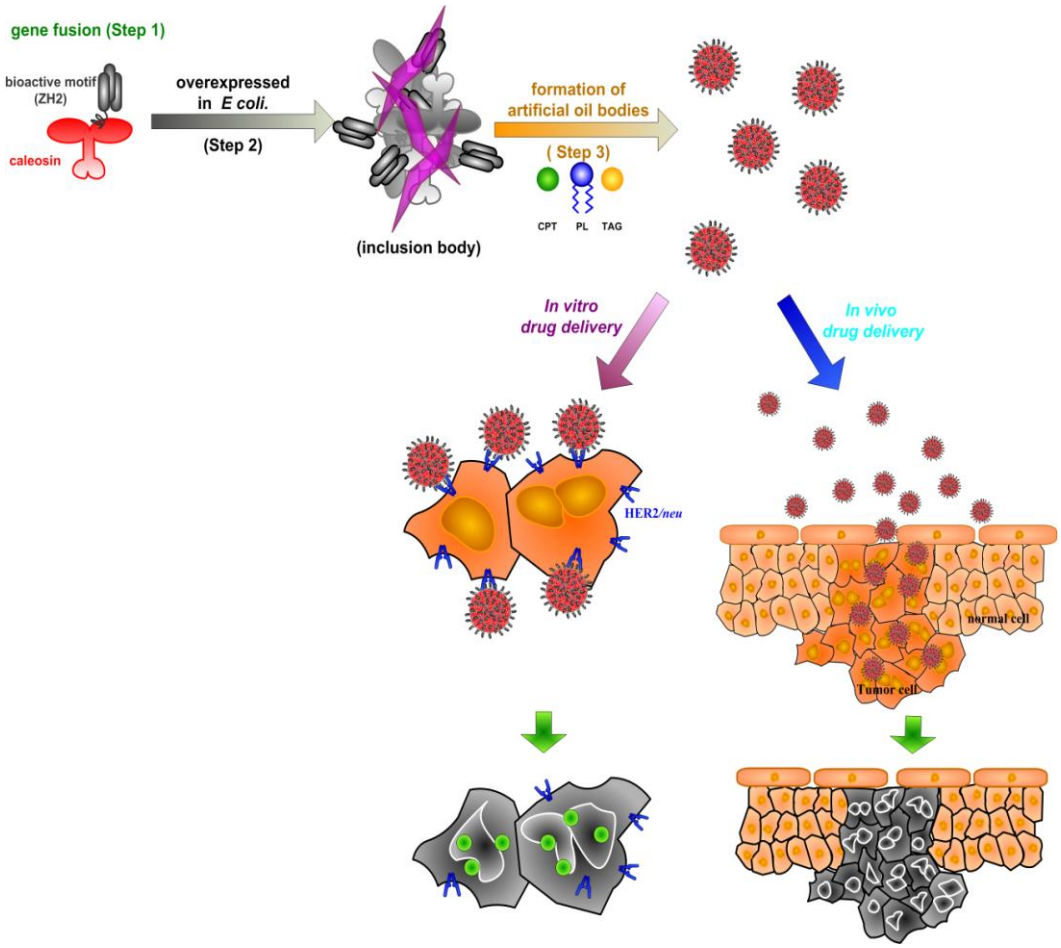
gene fusion (Step 1)
bioactive motif (ZH2)
caleosin
overexpressed in E coli.
(Step 2)
(inclusion body)
formation of artificial oil bodies
(Step 3)
CPT
PL
TAG
In vitro drug delivery
In vivo drug delivery
HER2/neu
normal cell
Tumor cell

Fig. 1

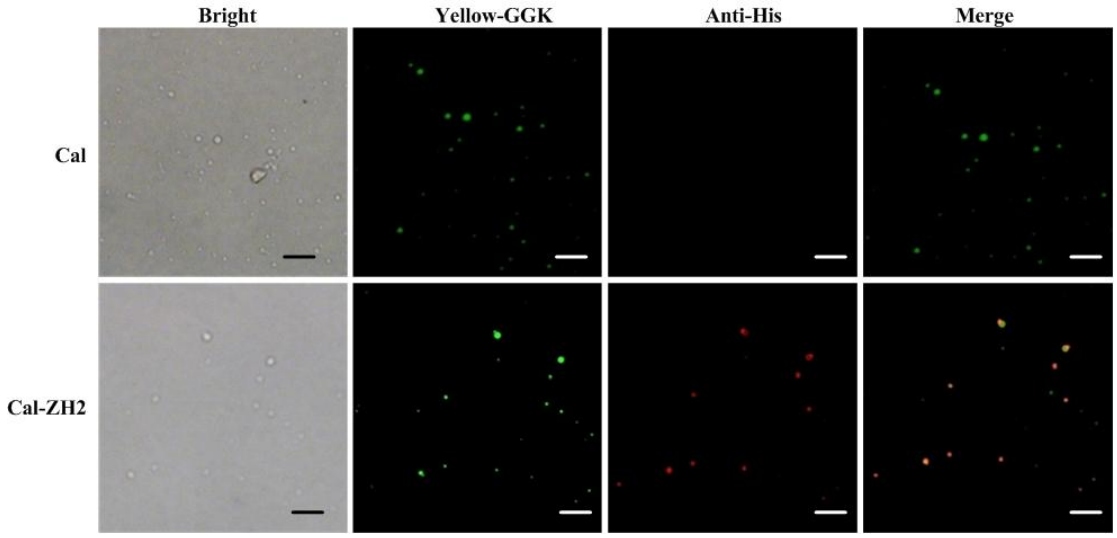
Bright
Yellow-GGK
Anti-His
Merge
Cal
Cal-ZH2

Fig. 2

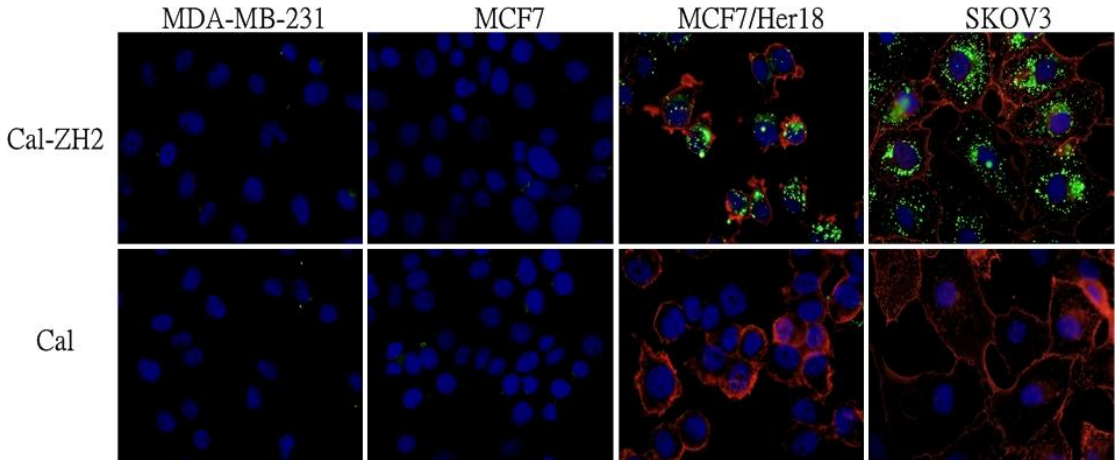
MDA-MB-231
MCF7
MCF7/Her18
SKOV3
Cal-ZH2
Cal

Fig. 3A

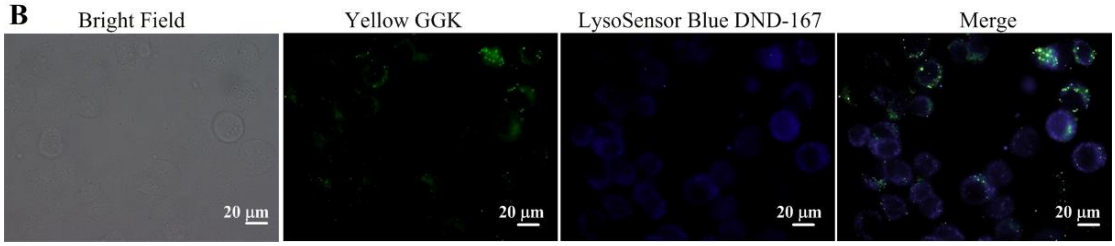
B
Bright Field
Yellow GGK
LysoSensor Blue DND-167
Merge
20 μm
20 μm
20 μm
20 μm

Fig. 3B

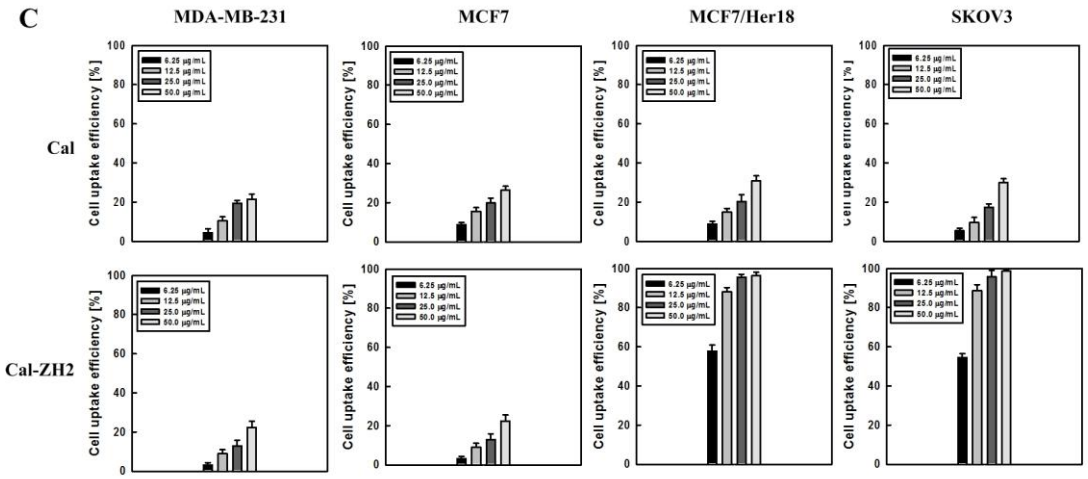

Fig. 3C

A

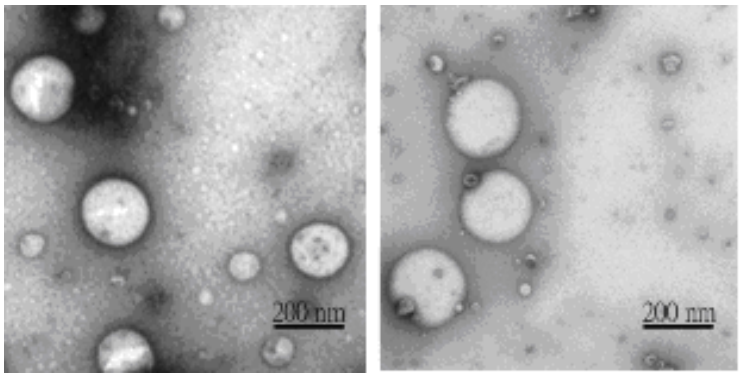

Fig. 4A

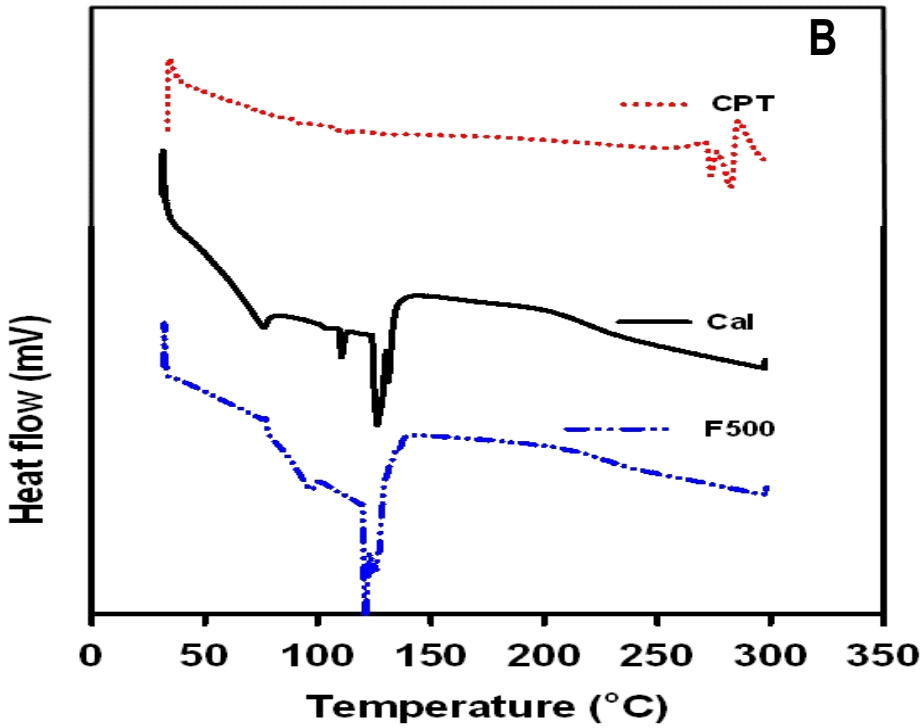
B
CPT
Cal
F500
Heat flow (mV)
0
50
100
150
200
250
300
350
Temperature (°C)

Fig. 4B

C

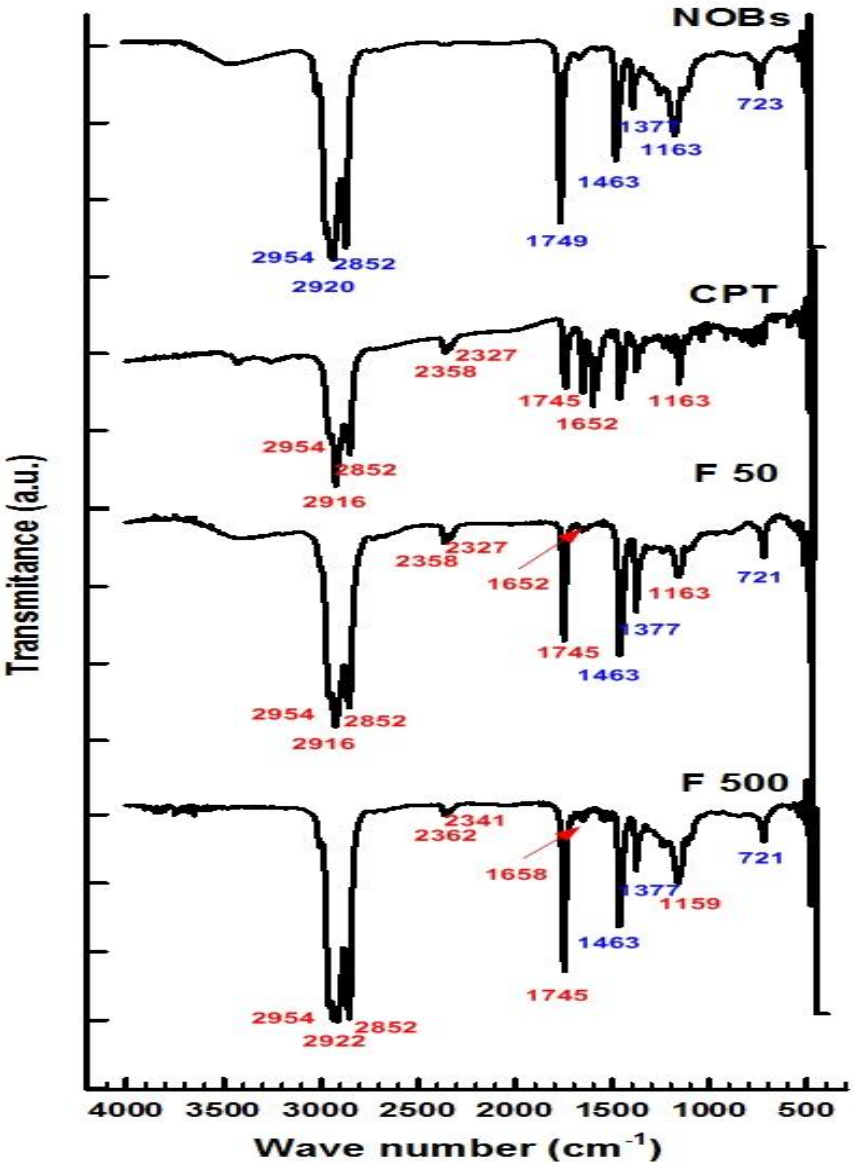
NOBs
723
1377
1163
1463
1749
2954
2852
2920
CPT
2327
2358
1745
1163
1652
2954
2852
2916
F 50
2327
2358
1652
721
1163
1377
1745
1463
2954
2852
2916
F 500
2341
2362
721
1658
1377
1159
1463
1745
2954
2852
2922
Transmitance (a.u.)
4000 3500 3000 2500 2000 1500 1000 500
Wave number (cm-1)

Fig. 4C

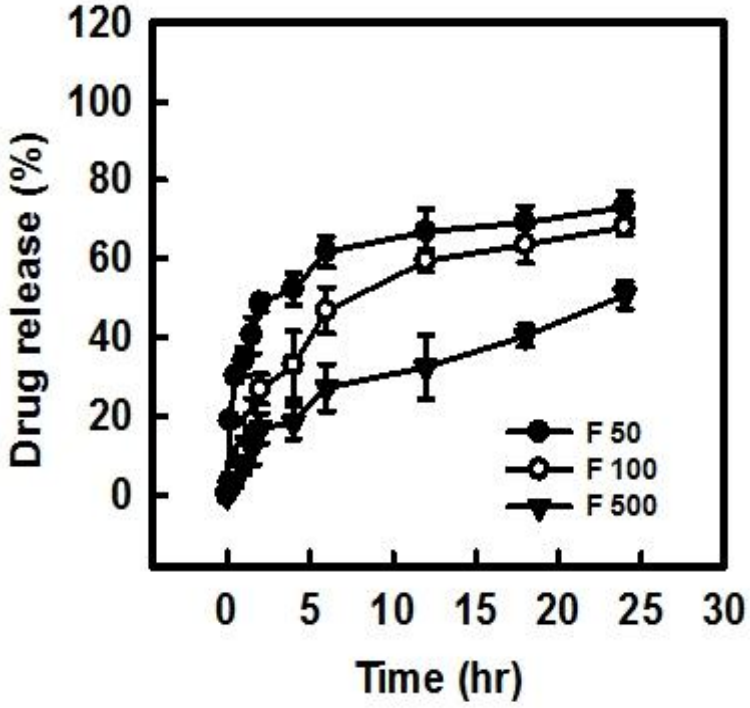
120
100
80
60
40
20
0
Drug release (%)
0
5
10
15
20
25
30
Time (hr)
F 50
F 100
F 500

Fig. 5

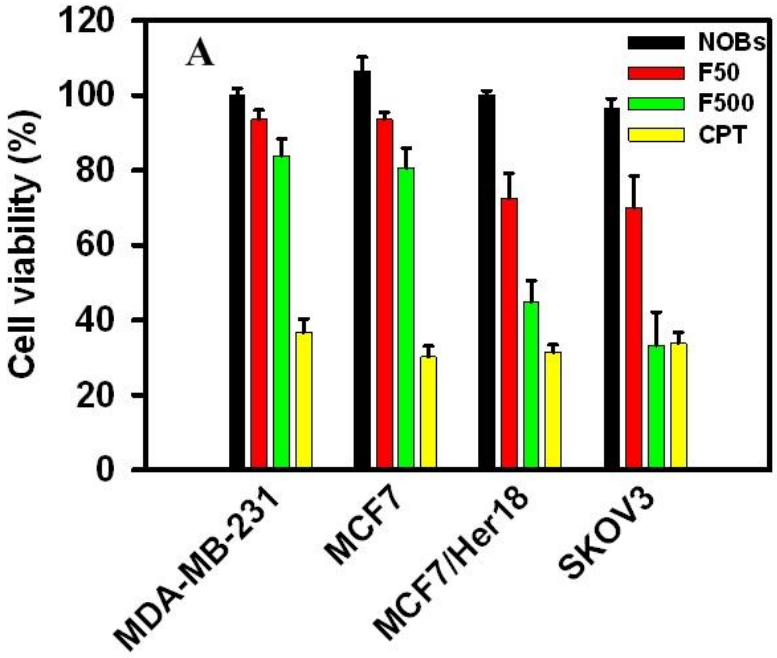
A
NOBs
F50
F500
CPT
Cell viability (%)
120
100
80
60
40
20
0
MDA-MB-231
MCF7
MCF7/Her18
SKOV3

Fig. 6A

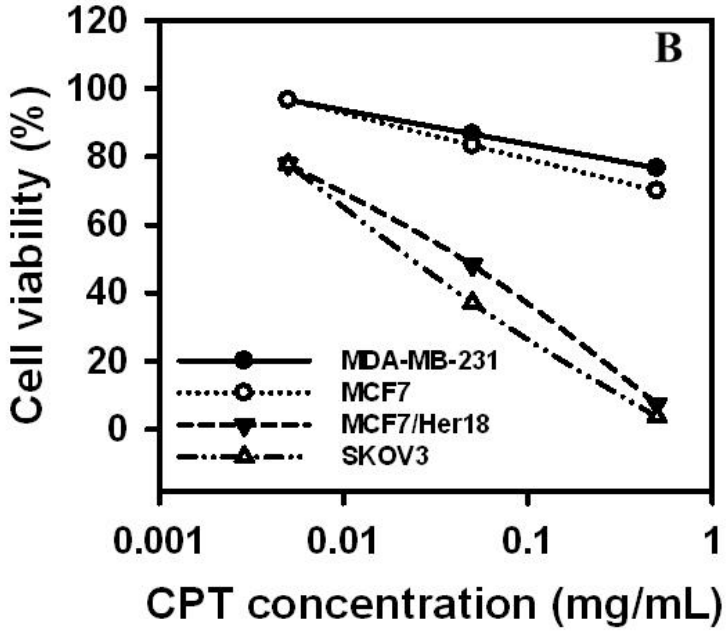
B
Cell viability (%)
120
100
80
60
40
20
0
MDA-MB-231
MCF7
MCF7/Her18
SKOV3
0.001
0.01
0.1
1
CPT concentration (mg/mL)

Fig. 6B

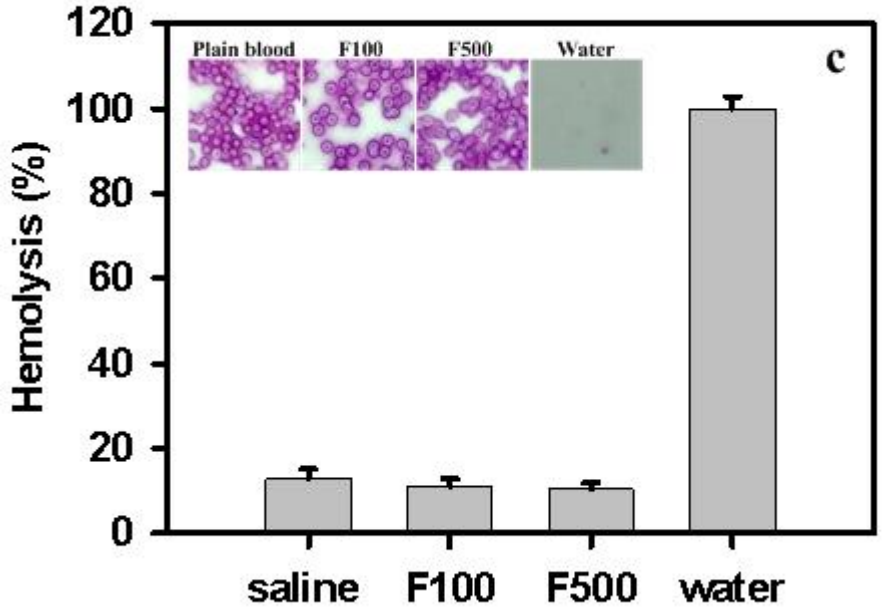
Plain blood
F100
F500
Water
c
Hemolysis (%)
120
100
80
60
40
20
0
saline
F100
F500
water

Fig. 6C

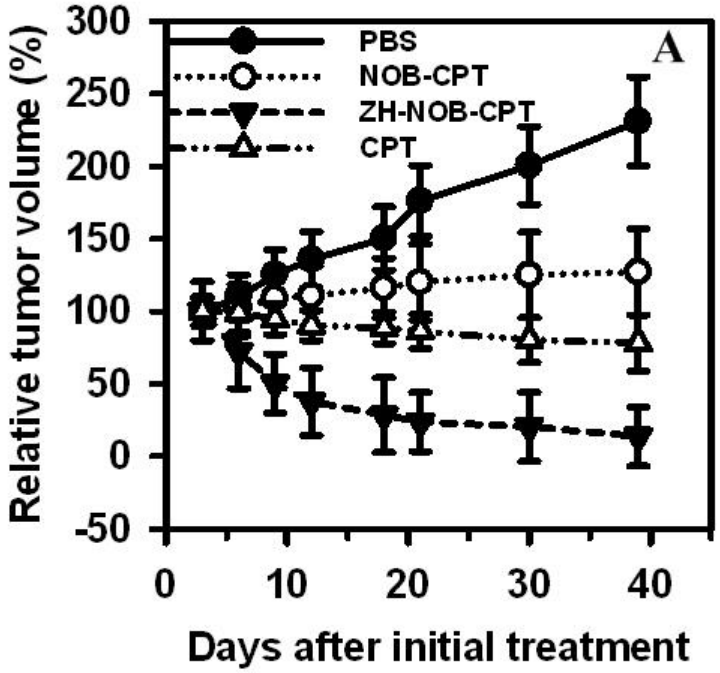
PBS
NOB-CPT
ZH-NOB-CPT
CPT
A
Relative tumor volume (%)
300
250
200
150
100
50
0
-50
0
10
20
30
40
Days after initial treatment

Fig. 7A

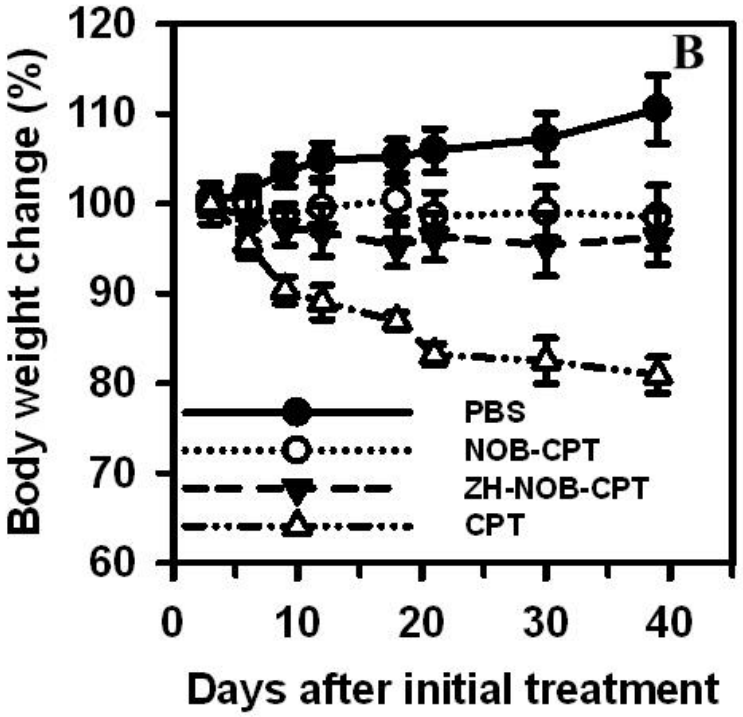
B
120
110
100
90
80
70
60
Body weight change (%)
0
10
20
30
40
Days after initial treatment
PBS
NOB-CPT
ZH-NOB-CPT
CPT

Fig. 7B